Indian Journal of Biochemistry & Biophysics
Vol. 59, February 2022, pp. 157-164

Anti-bacterial activity of neoandrographolide derivatives: *In silico* interaction with the bacterial target

Venu Sharma[1,2]*, Supriya Sharma[1], Rukmankesh Mehra[1], Kamal K Kapoor[3], Manoj K Dhar[1] & Sanjana Kaul[1]*

[1]School of Biotechnology & [3]Department of Chemistry, University of Jammu, Jammu 180 006, Jammu & Kashmir, India

[2]Indian Institute of Integrative Medicines, Jammu-180 001, Jammu & Kashmir, India

Received 05 November 2021; *revised 30 November 2021*

Natural products and their semi synthesized molecules have been used as efficient antibiotics since a long time. The present global health scenario has raised the demand for novel antimicrobial agents and drug targets that are effective against drug resistant pathogens, emerging infections *etc*. The current study has promoted the antibacterial activity of the glucoside labdane 'neoandrographolide', isolated from the methanolic extract of the medicinal plant *Andrographis paniculata*. Further modification at its glucoside hydroxyl groups to generate ester and acetonide derivatives was done and the antibacterial potential of these compounds was screened against common bacterial pathogens. Among various derivatives, 4′,6′-*O*-(4-methoxybenzylidene) neoandrographolide exhibited promising results. In addition, molecular modeling study of the active compound was also explored to identify its probable binding mode on the bacterial target. The present study reported antibacterial activity of neoandrographolide derivatives for first time and also the bioactive molecule, 4′,6′-*O*-(4-methoxybenzylidene) neoandrographolide was examined as a potent antibacterial agent against different strains.

Keywords: *Andrographis paniculata*, Antimicrobial activity, Labdane diterpenes, Molecular modeling, Semi-synthetic derivative

Anti-microbial compounds are of great importance due to the outbreak of newer infectious diseases, an increase in resistance of microorganisms against various drugs, and their harmful side effects. There is a need for the development of compounds with fewer side effects and more targeted activity on the microorganisms.[1] In the present study, neoandrographolide from an important medicinal plant, *Andrographis paniculata* (Burm.f.) Wall. ex Nees, was selected to explore its semi-synthetic derivatives and their antimicrobial potential[2].

Andrographis paniculata (commonly known as King of Bitters in English and as Kalmegh, Chirait in India) is a medicinal shrub. It is cited in Ayurveda, traditional Chinese medicines, and exhibits multiple pharmacological activities. The potent antibacterial property of the plant has been reported in literature[3-9]. The main phytoconstituents of the plant are labdane diterpenoids *viz.* andrographolide (potent anticancer agent), 14-deoxy-11,12-didehydroandrographolide, neoandrographolide *etc*[10-12]. Although andrographolide has been widely explored for its multiple pharmacological activities but very limited information is available on semi synthetic studies of the second principle phyto-constituent, 'neoandrographolide' of the plant. Neoandrographolide was at first isolated and characterized by Kleipool[10]. It is a labdane glucoside with molecular formula $C_{26}H_{40}O_8$, the molecular mass of 480.597 and has melting point 165-166°C. Its structure is comprised of C19-*O*-β-D-glucoside diterpene scaffold with α, β-unsaturated lactone moiety. It is soluble in methanol, ethanol, propanol, acetone, pyridine and acetic acid. Neoandrographolide has been reported as a more potent anti-inflammatory metabolite than andrographolide[13,14].

Based on our ongoing studies on isolation and semi-synthetic derivatization of labdane diterpenoids from *Andrographis paniculata*, it was envisaged to investigate the effect of carbohydrate modification in neoandrographolide to screen its biological activities. Our previous study reported the potential cytotoxicity of these derivatives. It was reported that modification at the carbohydrate moiety of neoandrographolide resulted in improved cytotoxicity against SW620, PC3 and A549 cell lines. The derivatives, 4′,6′-benzylidene neoandrographolide and 4′,6′-p-methoxybenzylidene neoandrographolide were observed as less toxic and more potent anticancer molecules[15]. It was planned to extend the study to

*Correspondence:
E-mail: venusharma80@gmail.com (VS); sanrozie@rediffmail.com (SK)

examine these semi-synthesized derivatives against different bacterial strains and it was found 4′,6′-O-(4-methoxybenzylidene)neoandrographolide (2c) was a potent antibacterial agent against different strains. Further, *in silico* study was executed to analyze the binding mode of the identified active neoandrographolide analogue and to provide initial information for further lead optimization of the hit.

Materials and Methods

The commercially available reagents were purchased from Sigma Aldrich and solvents from SD Fine Chemicals. The selected medicinal plant, *Andrographis paniculata* was obtained from the experimental plots of the School of Biotechnology, University of Jammu, Jammu. The plant material was taxonomically identified and the voucher specimen was deposited in the herbarium of the Department of Botany, the University of Jammu for future reference (Accession number: 15796).

Isolation of neoandrographolide and its semi-synthetic modifications

Shoot plant material (2.5 kg) of *A. paniculata* was shed, air- dried and macerated in methanol for 24 h. The extract was concentrated and the mass (128 g) was subjected to liquid-liquid partitioning with different solvents (hexane, dichloromethane , and methanol). Neoandrographolide (3 g) was isolated as white needle like crystals with melting point 174-175°C. It was chemically identified as *ent*-19-hydroxy-8(17), 13-labdadien-16,15-olide 19-*O*-β-D-glucopyranoside based on the comparison of its spectral data (^{1}H, ^{13}C, Mass, IR) with that reported in the literature[10]. Neoandrographolide (1) was transformed into 4′,6′-protected acetals [2 (a-c)] and its tetra acetyl (3) and tetrabenzoate (4) derivatives at room temperature (RT) as depicted in (Fig. 1) by our previously reported method[16]. The neoandro grapholide derivatives, modified at the carbohydrate site, were confirmed by spectral analysis[15]. All the derivatives and the parent compound were evaluated for antibacterial activity.

Assessment of antimicrobial activity

Antimicrobial activity of the parent compound and its derivatives against common bacterial pathogens was determined on Müller-Hinton Agar (MHA) media (Himedia, India) using a well diffusion technique with slight modifications[17]. A total of eight pathogenic bacterial strains including four gram-positive and four gram- negative bacteria were used in the antibacterial assays. The bacterial strains were procured from Microbial Type Culture Collection and gene bank (MTCC), Institute of Microbial Technology (IMTECH), Chandigarh. The bacterial strains included *Pseudomonas aeruginosa* (MTCC-1934), *Bacillus subtilis* (MTCC-441), *Klebsiella*

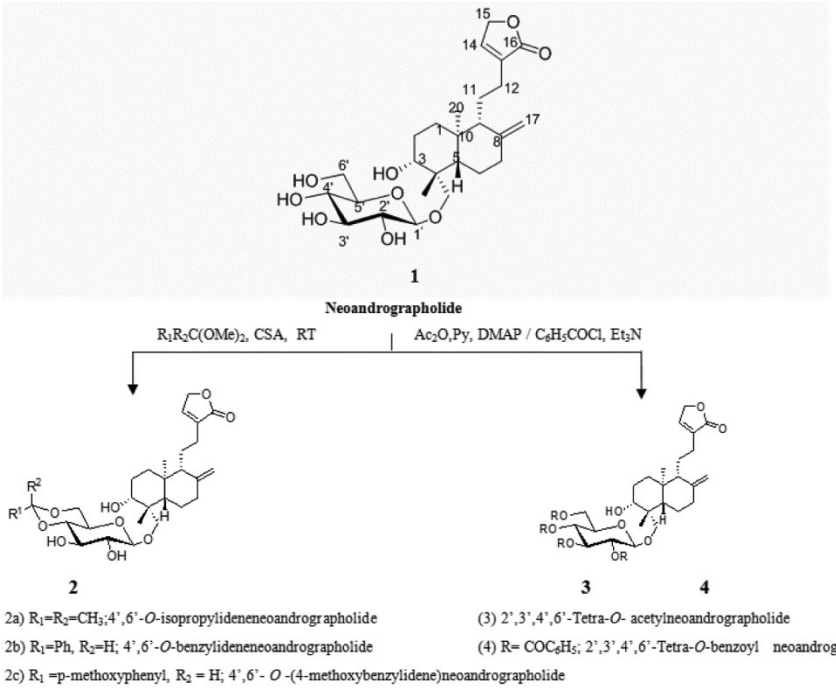

Fig. 1 — Semi synthetic acetal and ester derivatives of neoandrographolide

pneumonia (MTCC-109), *Pseudomonas alcaligenes* (MTCC-493), *Staphylococcus aureus* (MRSA), *Enterococcus faecalis* (MTCC-439*), Bacillus cereus* (MTCC-430*)* and *Escherichia coli* (MTCC-40). Suspensions of the bacterial strains were prepared from cells arrested during their logarithmic growth phase (18 h) on Nutrient Broth (NB) at 37°C. The concentration of the bacterial suspension was adjusted spectrophotometrically at 620 nm wavelength and adjusted to an optical density (OD) of 0.5 with saline and 0.5 McFarland standard (equivalent to 1.5×10^8 CFU/mL).

The parent compound and its derivatives were dissolved in Dimethyl sulphoxide (DMSO) at a concentration of 1 mg/mL. The bacterial suspension was spread over MHA plates and specific numbers of wells were punched with a sterile cork borer (8 mM diameter) in each plate. 100 µL of various concentrations of the test compounds along with both positive and negative control were added into wells. DMSO was taken as negative control and standard antibiotic chloramphenicol (100 µg/mL concentration) was taken as a positive control. The plates were allowed to stand for 1 h for the diffusion of the extracts followed by incubation for 24 h at 37 ± 2°C. The antibacterial potential of the test compounds was determined in terms of the diameter of the clear bactericidal zone around the well. The compounds showing a clear zone around the well were considered as positive whereas those not showing a clear zone around the well were considered as negative. The compounds with potential antibacterial activity (based on the significant diameter of clear zone) were further selected for the determination of Minimal Inhibitory Concentration (MIC). MIC was determined using the same methodology as given above with slight modifications[11]. Various dilutions of the test compounds ranging from 1000 - 100 µg/mL (1000, 800, 500, 300, 200, 100 µg/mL) or further lower concentrations, if required (80, 60, 40, 20 µg/mL) were used for determination of MIC.

Molecular modeling studies

The amino acid sequence of *B. cereus* (MTCC - 430) ICDH was retrieved from UniProtKB database[17] and its structure was modeled using Modeller software[19,20]. The modelled structure was validated using Ramachandran plot analysis and structure alignment with the template structure. The analysis of the Ramachandran plot was done using Ram Page server[20]. To further carryout the docking studies, the predicted protein structure as well as ligand were prepared and subjected to docking analysis using Auto Dock Vina software[19]. Visualization of the results was performed using Pymol[21] and Poseview tools[22].

Results

In the current study, assessment of antibacterial activity revealed that the parent compound, neoandrographolide, and some of its derivatives possessed potential activity against one or more pathogens. The compounds with potential activity at the concentration of 1 mg/mL, were further selected for the determination of MIC. Among all the derivatives, improved antimicrobial activity of 4′,6′-*O*-p-methoxybenzyledene neoandrographolide (2c) was observed against *B. subtilis* and *B. cereus*. A significant increase in the antimicrobial potential of

Table 1 — Antibacterial activity of neoandographolide and its derivatives against various pathogens

	Compounds							
	A	B	C	D	E	F	G	H
Pathogens	Diameter of clear zone (mm): (Fold Increase %)							
Bacillus cereus	15	12: (−20)	10: (−33.33)	nil	19: (26.67)	nil	21: (40)	nil
Bacillus subtilis	12	nil	nil	nil	14: (16.67)	nil	20: (66.67)	nil
Enterococcus faecalis	13	10: (−23.07)	nil	nil	12: (−7.69)	nil	19: (46.15)	nil
Staphylococcus aureus	14	13: (−7.14)	nil	11: (−21.43)	10: (−28.57)	nil	20: (42.85)	nil
Pseudomonas aeruginosa	10	nil	9: (−10)	10: (0)	nil	nil	24: (140)	nil
Pseudomonas alcaligenes	13	10: (−23.07)	nil	nil	nil	9: (−30.77)	24: (84.61)	nil
Escherichia coli	10	9: (−10)	nil	10: (0)	11: (10)	nil	23: (130)	nil
Klebsiella pneumonia	12	nil	nil	nil	nil	11: (−8.33)	19: (58.33)	nil

where, A: Neoandographolide (1); B: 4′,6′-*O*-isopropylidene neoandrographolide (2a); C: 4′,6′-*O*-benzylidene neoandrographolide (2b); D:2′,3′,4′,6′-Tetra-*O*-acetylneoandrographolide; E: 4′,6′-*O*-4-methoxybenzylidene neoandrographolide (2c); F: 2′,3′,4′,6′-Tetra-*O*-benzoylneoandrographolide; G: +ve control chloramphenicol; H: −ve control DMSO

4′,6′-*O*-p-methoxybenzyledene neoandrographolide (2c) with respect to the activity of the parent compound was observed against *B. cereus*. (Table1). Evaluation of MIC of 4′,6′-*O* -(4-methoxy benzyledene) neoandrographolide reported that it inhibited the pathogen *B.cereus* upto the lower concentration of 80 µg/mL. This concentration was significantly lower than the MIC of the parent molecule for which the inhibition against all the pathogens ranged from 100-300 µg/mL (Table 2).

Structure prediction, model validation ,and docking studies

The molecular modeling study of the active compound identified in the current study was done in order to analyze its mode of binding at the target binding site. It has been reported that the proteins isocitrate dehydrogenase (ICDH) and amino glycoside 2′-N-acetyltransferase (AAC) are the probable targets of andrographolide[23]. Since no protein structure as well as sequence of *B. cereus* AAC was available in the literature, the binding mode studies of the identified active compound 2c**,** (4′,6′-*O*-4-methoxybenzyledene neoandrographolide) was done only against ICDH. For homology modeling of the *B. cereus* ICDH, its sequence was retrieved from UniProtKB database (UniProt ID: A0A063CNL2)[24]. The search of this sequence against PDB database[25] using BLASTP program[17] revealed the presence of a highly identical protein structure 1HQS in PDB[25] that shared a percentage sequence identity of 86% and similarity of 92% with query coverage of 98% with the target sequence A0A063CNL2. The chain A of the PDB structure 1HQS was then used as a template for modeling the 3D-structure of the *B. cereus* ICDH. The sequence alignment of *B. cereus* ICDH was done with the template and five structural models were built using modeller software[26]. In order to validate the modeled structures, the stereo chemical analysis of the models was performed using the Ramachandran plot. The model with the highest number of residues in the favored region and the least number of residues in the outlier region was selected for further analysis (Fig. 2). The selected model showed 97.4% residues in the favored region and 0.9% residues in the outlier region (Fig. 2A). To further validate the modeled structure, the structural alignment of this model was done with the template 1HQSA. The structural alignment showed a RMSD of 0.352Å (Fig. 2B), which indicated a high structural similarity of the modeled structure with the template.

Table 2 — MIC of neoandographolide and its derivatives against various pathogens

Pathogens	Compounds	Concentration (µg/mL)								
		100	800	500	300	200	100	80	G	H
		Diameter of clear zone (in mm): (Fold Increase %)								
Klebsiella pneumonia	A	12	11	10	9	nil	nil	nil	19	nil
	F	11: (−8.33)	9: (−18.18)	nil	nil	nil	nil	nil	19	nil
Pseudomonas alcaligenes	A	14	13	12	11	10	10	nil	24	nil
	B	10: (−28.57)	nil	nil	nil	nil	nil	nil	24	nil
	F	9: (−35.71)	nil	nil	nil	nil	nil	nil	24	nil
Enterococcus faecalis	A	13	12	11	11	9	nil	nil	19	nil
	B	10: (−23.07)	nil	nil	nil	nil	nil	nil	19	nil
	E	12: (−7.69)	10: (−16.66)	nil	nil	nil	nil	nil	19	nil
Bacillus subtilis	A	12	12	11	9	nil	nil	nil	22	nil
	E	14: (16.66)	13: (8.33)	12: (8.33)	10: (8.33)	nil	nil	nil	22	nil
Bacillus cereus	A	15	14	12	11	9	nil	nil	21	nil
	B	12: (−20)	11: (−21.43)	9: (−25)	nil	nil	nil	nil	21	nil
	C	10: (−33.33)	10: (−28.57)	nil	nil	nil	nil	nil	21	nil
	E	19: (26.66)	17 : (21.42)	15: (25)	14: (27.27)	13: (44.44)	11	10	21	nil
Staphylococcus aureus	A	14	12	11	nil	nil	nil	nil	20	nil
	B	13: (−7.14)	12	10: (−9.09)	10	nil	nil	nil	20	nil
	D	11: (−21.42)	9: (−25)	nil	nil	nil	nil	nil	20	nil
	E	10: (−28.57)	nil	nil	nil	nil	nil	nil	20	nil

where, G: +ve control chloramphenicol; H: −ve control DMSO

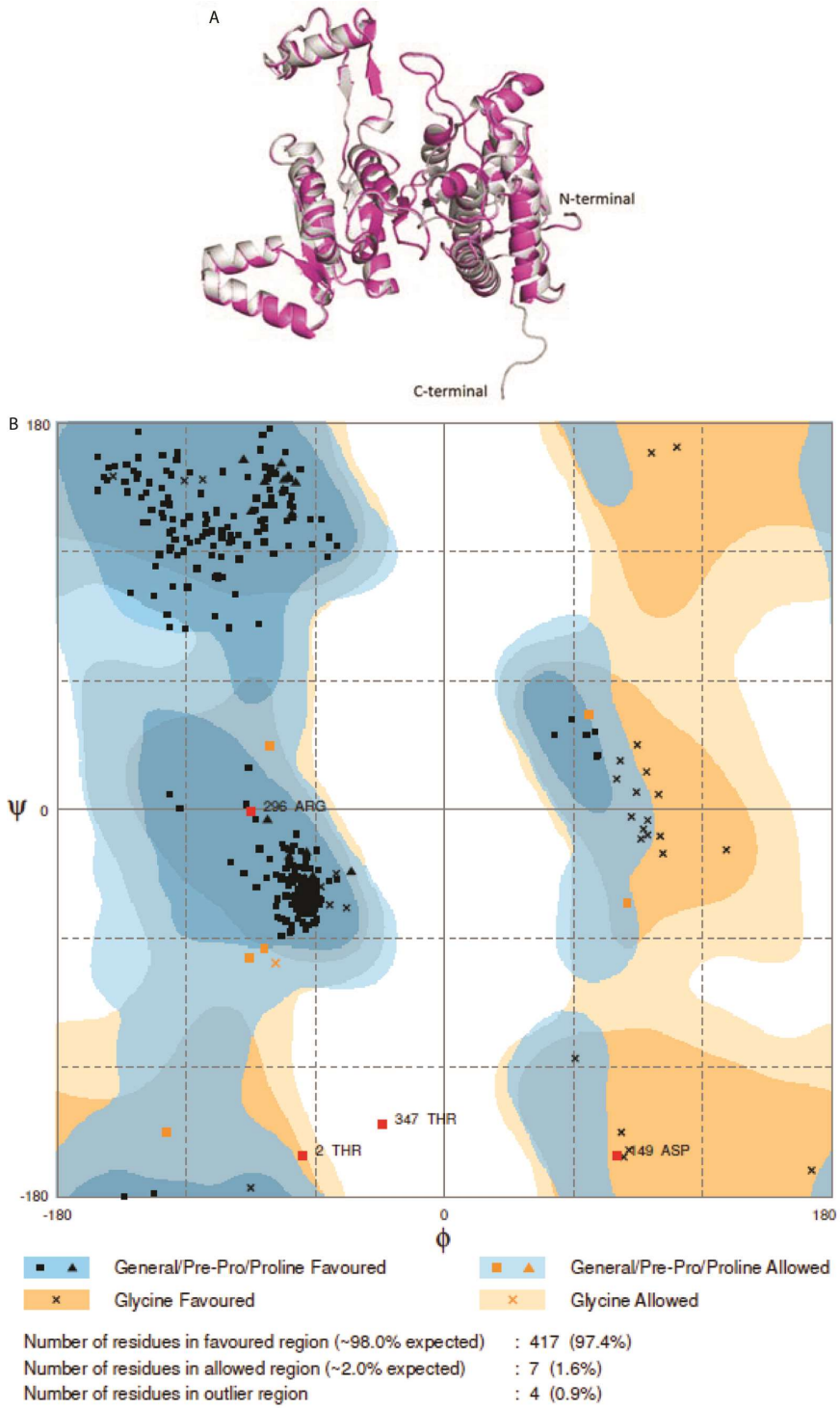

Fig. 2 — Homology modeled structure of *B. cereus* ICDH using PDB structure 1HQS as template. (A) Cartoon representation of the structurally aligned proteins of the built model of *B. cereus* ICDH (grey color) and the template 1HQS (magenta color). (B) Ramachandran plot of the modeled *B. cereus* ICDH structure.

For docking studies, polar hydrogen atoms were added to the ICDH model, H-bonds were calculated, and minimization of the protein was performed to remove any steric clashes using Swiss PDB viewer[20]. In order to identify the binding site, the ligand coordinates were copied from 1HQSA to the ICDH model. A 3D grid was generated at substrate (citric acid) binding site, and the compound 2c was docked

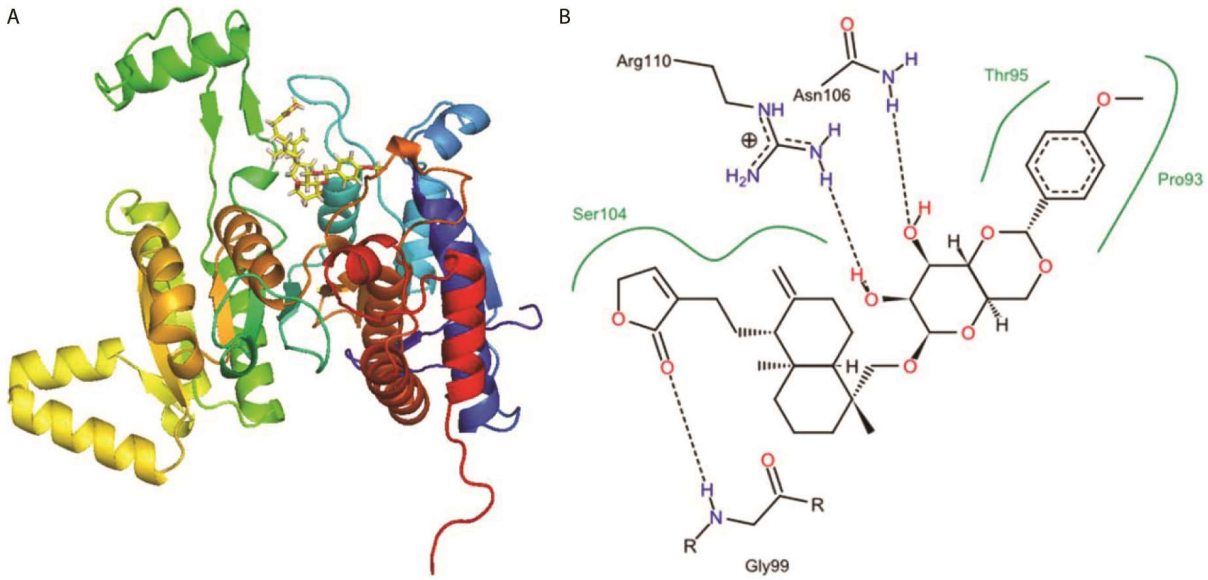

Fig. 3 — Mode of binding of compound (2c). (A) Docked pose of the compound (2c) (represented as stick model with yellow colored carbons) at the binding pocket of the *B. cereus* ICDH model. (B) Residues of the *B. cereus* ICDH binding site interacting with compound (2c)

on the generated grid using Auto Dock Vina[27]. The ligand structure was drawn using Chem Draw and converted to 3D using ChemBio3D.

Discussion

The current study, the parent compound was found to be more effective against gram -positive bacteria than gram -negative bacteria. One of the possible reasons behind this can be the composition of the bacterial cell wall. Gram-negative bacteria have a thin lipopolysaccharide exterior membrane that acts as an effective permeability barrier and thereby restricts the penetration of the compounds. In gram-positive bacteria, a mesh-like peptidoglycan layer is present that is permeable to compounds[28].

Likewise, the derivatives of neoandrographolide exhibited inhibition potential against gram positive bacteria. Among various derivatives, 4′,6′-*O*-(4-methoxybenzyledene) neoandrographolide was found to possess enhanced activity against *B. subtilis* and *B. cereus* as compared to its parent compound. The effectiveness can be attributed to certain structural modifications that might increase the effectiveness of the compounds. The polarity of compounds might be a probable reason for differential susceptibility of the tested compound[29].

Broad spectrum antimicrobial activity of andrographolide and other compounds, 3-O-β-D-glucosyl-14-deoxyandrographolide and 14-deoxy andrographolide isolated from *A. paniculata* has been reported[7]. Similarly, the study conducted by Rashid *et al*. (2018) reported the antimicrobial potential of 14-deoxyandrographolide against gram negative bacteria[30]. Although, antimicrobial potential of various diterpene phytoconstituents of *A. paniculata* has been mentioned against different species of the *Bacillus* genus reports on antimicrobial potential against *B. cereus* are seldom available.

In docking studies, the docked pose of the compound 2c at the protein binding site was analyzed so as to identify crucial protein-ligand interactions (Fig. 3). It was observed that the residues Gly99, Asn106 and Arg110 were involved in H-bonding interactions with the ligand, and all these residues were found to be H-bond donors (Fig. 3B). The backbone NH of the Gly99 formed H-bond with the carbonyl oxygen atom of the furanone ring of the ligand. The side chain NH_2 group of the Asn106 residue was found to form H-bonding interaction with the OH group of the ligand. The side chain NH_2 of the guanidine group of Arg110 formed H-bond interaction with the hydroxyl group of the ligand. The guanidium group of Arg110 also showed a tendency to involve in salt-bridge interaction with the ligand. Apart from these, residues Pro93, Thr95, and Ser104 were also found to form important interactions with the ligand (Fig. 3B). The benzene ring of the anisole group of the ligand formed hydrophobic interactions with the target binding site (Fig. 3B).

Further, the drug-like properties of compound (2c) were studied using FAFDrugs4 server[31]. Compound (2c) exhibited logP value of 4.32, total polar surface

area of 112.19 and good VEBER oral bioavailability. The number of H-bond donors and acceptors were 2 and 9, respectively.

Conclusion

Neoandrographolide, a major 19-*O*-β-glucoside labdane of *A. paniculata* was derivatized to its glycosyl hydroxyl- protected molecules. These analogues were assessed for their antibacterial potential as compared to the parent molecule. An increase in antibacterial activity was observed in 4′,6′-*O*-(4-methoxybenzyledene)neoandrographolide. The binding mode study of the identified antibacterial derivative on the target ICDH, identified three essential residues *viz*. Gly99, Asn106 and Arg110, which were involved in H-bonding interactions with the compound. To the best of our knowledge, this is the first report on antibacterial study of 19-*O*-β-glucoside analogues of neoandrographolide.

Acknowledgement

The authors would like to acknowledge Director, School of Biotechnology and Coordinator, Bioinformatics Centre, School of Biotechnology, University of Jammu for facilities. VS would like to thank Department of Science and Technology, Government of India for funding under WOS-A projects [SR/WOS-A/CS-111/2013, SR/WOS-A/CS-46/2018]. Department of Biotechnology, Govt. of India is also acknowledged for funding and facilities

Conflict of interest

All authors declare no conflict of interest.

References

1 Singh R, Prasad J, Satapathy T, Jain P & Singh S, Pharmacological evaluation for anti-bacterial and anti-inflammatory potential of polymeric microparticles. *Indian J Biochem Biophys*, 58 (2021) 156.

2 Murugan NA, Pandian CJ & Jeyakanthan J, Computational investigation on *Andrographis paniculata* phytochemicals to evaluate their potency against SARS-CoV-2 in comparison to known antiviral compounds in drug trials. *J Biomol Struct Dyn*, 39 (2021) 4415.

3 Mishra K, Dash AP, Swain BK & Dey N, Anti-malarial activities of *Andrographis paniculata* and *Hedyotis corymbosa* extracts and their combination with curcumin. *Malar J*, 8 (2009) 26.

4 Radhika P & Lakshmi KR, Antimicrobial activity of the chloroform extracts of the root and the stem of *Andrographis paniculata* Nees. *Int Res J Microbiol*, 1 (2010) 37.

5 Roy S, Rao K, Bhuvaneswari C, Giri A & Mangamoori LN, Phytochemical analysis of *Andrographis paniculata* extract and its antimicrobial activity. *World J Microbiol Biotechnol*, 26 (2010) 85.

6 Singha PK, Roy S & Dey S, Antimicrobial activity of *Andrographis paniculata*. *Fitoterapia*, 74 (2003) 692.

7 Sule A, Ahmed QU, Latip J, Samah OA, Omar MN, Umar A & Dogarai BBS, Antifungal activity of *Andrographis paniculata* extracts and active principles against skin pathogenic fungal strains in vitro. *Pharm Biol*, 50 (2012)850.

8 Hossain S, Urbi Z, Karuniawati H, Mohiuddin RB, Moh Qrimida A, Allzrag AMM, Ming LC Pagano E & Capasso R, *Andrographis paniculata* (Burm. F.) Wall. Ex Nees: An updated review of phytochemistry, antimicrobial pharmacology, and clinical safety and efficacy. *Life*, 11 (2021) 4.

9 Zhang L, Bao M, Liu B, Zhao H, Zhang Y, Ji X, Zhao N, Zhang C, He X, Yi J, Tan Y, Li L & Lu C, Effect of andrographolide and its analogs on bacterial infection: A review. *Pharmacology*, 105 (2020) 123.

10 Kleipool RJC, Constituents of *Andrographis paniculata* Nees. *Nature*, 169 (1952) 33.

11 Sharma V, Sharma T, Kaul S, Kapoor KK & Dhar MK, Anticancer potential of labdane diterpenoid lactone "andrographolide" and its derivatives: a semi-synthetic approach. *Phytochem Rev,* 16 (2017) 513.

12 Murthy HN & Dalawai D, Biotechnological production of diterpenoid lactones from cell and organ cultures of *Andrographis paniculata*. *Appl Microbiol Biotechnol*, 27 (2021) 1.

13 NNNR, Furuta T, Kojima S, Takane K & Ali Mohd M, Antimalarial activity of extracts of Malaysian medicinal plants. *J Ethnopharmacol*, 64 (1999) 249.

14 Bhat MA & Murthy HN, Isolation, Characterization of Neoandrographolide from *Andrographis macrobotrys* Nees and Evaluation of its effect on LPS induced TNF-α Activity. *Pharmacogn J*, 13 (2021) 669.

15 Sharma V, Qayum A, Kaul S, Singh A, Kapoor KK, Mukherjee D, Singh SK & Dhar MK, Carbohydrate modifications of Neoandrographolide for improved reactive oxygen species-mediated apoptosis through mitochondrial pathway in colon cancer. *ACS Omega*, 4 (2019) 20435.

16 Sharma V, Kapoor KK, Mukherjee D, Gupta VK, Dhar MK & Kaul S, Camphor sulphonic acid mediated quantitative 1,3-diol protection of major Labdane diterpenes isolated from *Andrographis paniculata. Nat Prod Res*, 32 (2018) 1751.

17 Schwalbe R, Steele-Moore L & Goodwin AC, Antimicrobial susceptibility testing protocols. *CRC Press Taylor & Francis group*, (2007) 414.

18 Altschul SF, Gish W, Miller W, Myers EW & Lipman DJ, Basic local alignment search tool. *J Mol Biol*, 215 (1990) 403.

19 Kaplan W & Littlejohn TG, Swiss-PDB Viewer (Deep View). *Brief Bioinform*, 2 (2001) 195.

20 Lovell SC, Davis IW, Arendall III WB, de Bakker PIW, Word JM, Prisant MG, Richardson JS & Richardson DC, Structure validation by Cα geometry: ϕ, ψ and Cβ deviation. *Proteins: Struct, Funct, and Bioinfo*, 50 (2003) 437.

21 Delano WL, Pymol: An open-source molecular graphics tool. *CCP4 Newsletter on protein crystallo*, 40 (2002) 82.

22 Stierand K, Maass PC & Rarey M, Molecular complexes at a glance: automated generation of two-dimensional complex diagrams. *Bioinformatics*, 22 (2006) 1710.

23 Prabu A, Hassan S, Shainaba AS, Hanna LE & Kumar V, Andrographolide: A potent antituberculosis compound that targets Aminoglycoside 2′-N-acetyltransferase in *Mycobacterium tuberculosis*. *J Mol Graph*, 61 (2015) 133.
24 Consortium U, Reorganizing the protein space at the universal protein resource (uniprot). *Nucleic Acids Res*, 40 (2012) D71.
25 Berman HM, Battistuz T, Bhat TN, Bluhm WF, Bourne PE, Burkhardt K, Feng Z, Gilliland GL, Iype L & Jain S, The protein data bank. *Acta Crystallogr D Biol Crystallogr*, 58 (2002) 899.
26 Sali A, Potterton L, Yuan F, van Vlijmen. H & Karplus M, Evaluation of comparative protein modeling by MODELLER. *Proteins*, 23 (1995) 318.
27 Trott O & Olson AJ, Autodock Vina: improving the speed and accuracy of docking with a new scoring function, efficient optimization, and multithreading. *J Comput Chem*, 31 (2010) 455.
28 Sharma S, Gupta S, Dhar MK & Kaul S, Diversity and bioactive potential of culturable fungal endophytes of medicinal shrub *Berberis aristata* DC.: A first report. *Mycobiology*, 46 (2018) 370.
29 Arifullah M, Namsa ND, Mandal M, Chiruvella KK, Vikrama P & Gopal GR, Evaluation of anti-bacterial and anti-oxidant potential of andrographolide and echiodinin isolated from callus culture of *Andrographis paniculata* Nees. *Asian Pac J Trop Biomed*, 3 (2013) 604.
30 Rashid PT, Ahmed M, Rahaman MM & Muhit MA, 14-Deoxyandrographolide isolated from *Andrographis paniculata* (Burm. F) Nees Growing in Bangladesh and its Antimicrobial Properties. *Dhaka Univ J Pharm Sci*, 17 (2018) 265.
31 Miteva MA, Violas S, Montes M, Gomez D, Tuffery P & Villoutreix BO, FAF-Drugs: free ADME/tox filtering of compound collections. *Nucleic Acids Res*, 34 (2006) W738.